Fuel Cells

DOI: 10.1002/anie.201003261

Ternary Heterostructured Nanoparticle Tubes: A Dual Catalyst and Its Synergistic Enhancement Effects for O_2/H_2O_2 Reduction**

*Chun-Hua Cui, Hui-Hui Li, Jin-Wen Yu, Min-Rui Gao, and Shu-Hong Yu**

The ability to control the chemical composition and the interface structure of multicomponent heterogeneous metallic catalysts without the support of porous carbon materials and foreign oxides is a challenging catalyst design area and can be aided by understanding the respective function of the metallic components. Generally, the alloy surface has an unusual electronic structure and arrangement of surface atoms in the near-surface region. A monolayer of noble metals, such as Pt or Pd,[1] deposited on a host metal or alloy may induce strain and ligand effects, which can improve the activities.[2] The promising strategies to change activities concern introducing a guest metal to form near-surface alloys and heterogeneous interfaces[3] that endow the surface and interface with improved catalytic properties.[3a,c,4] However, the active metals, including Au, Fe, Ni, Cu, are usually alloyed or protected by noble metal layer, the naked-state effect of these active metals on the catalytic activity is unknown, but it is fascinating because of the unique interface and different oxidation state of the active metal.

Recently, some research work focused on the unique catalytic activity of dispersed metal nanoparticles supported on oxides and the metal/oxide support interface boundary sites has provided evidence for the enhancement of the catalytic activity.[5] However, these support oxides are usually impossible to reverse, which means that the oxides cannot be reduced into metallic state, and the oxidation state cannot be adjusted. Herein, we describe a Pd-Au/CuO@Cu heterostructured nanoparticle tube (HNT) catalyst, in which the CuO layer can be formed at lower potential when a metal (gold) component is added into the bimetallic PdCu system. The CuO layer formation is aided by the potential difference of the Au/Cu system. At negative potential, the CuO layer can be reduced and the PdAuCu catalyst is restored.

[*] Dr. C.-H. Cui, H.-H. Li, J.-W. Yu, Dr. M.-R. Gao, Prof. Dr. S.-H. Yu
Division of Nanomaterials & Chemistry, Hefei National Laboratory for Physical Sciences at Microscale, Department of Chemistry
University of Science and Technology of China
Hefei 230026 (P.R. China)
Fax: (+86) 551-360-3040
E-mail: shyu@ustc.edu.cn
Homepage: http://staff.ustc.edu.cn/~yulab/

[**] This work was supported by the National Basic Research Program of China (2010CB934700), the National Natural Science Foundation of China (NSFC, Nos. 91022032 and 50732006), International Science & Technology Cooperation Program of China (2010DFA41170), and the Principle Investigator Award by the National Synchrotron Radiation Laboratory at the University of Science and Technology of China.

Supporting information for this article is available on the WWW under http://dx.doi.org/10.1002/anie.201003261.

The PdAuCu HNT was synthesized by a facile, non-aqueous solution electrodeposition method.[6] Unlike the seeded-growth method or metallic-precursor reduction[3c,7] for the synthesis of heterostructure nanoparticle materials, which require a mass of surfactants that will hinder the catalytic activity of metal surface, this strategy just uses dimethyl sulfoxide (DMSO) as a solvent and as a surfactant, which is bound to the metal surface by the sulfur atom in an inverted pyramid configuration and can be washed away easily owing to it weak absorption on the surface.

We synthesized a family of PdAuCu HNT catalysts by a one-step electrodeposition route onto an anodic aluminum oxide (AAO) template in anhydrous DMSO solution without the addition of any other surfactants (see Supporting Information). The aim of designing a tubular structure is to enhance the performance durability, eliminate the support-effect problem, and relax the Ostwald ripening and aggregation in contrast to the situation for particles.[8] The scanning electron microscopy (SEM) images in Figures 1a and 1b show that the as-synthesized PdAuCu HNTs have lengths of several micrometers and a diameter of about 300 nm. The PdAuCu HNTs were completely dispersed and provided a three-dimensional space for the mass transfer of O_2 and H_2O_2 molecules. A typical transmission electron microscopy

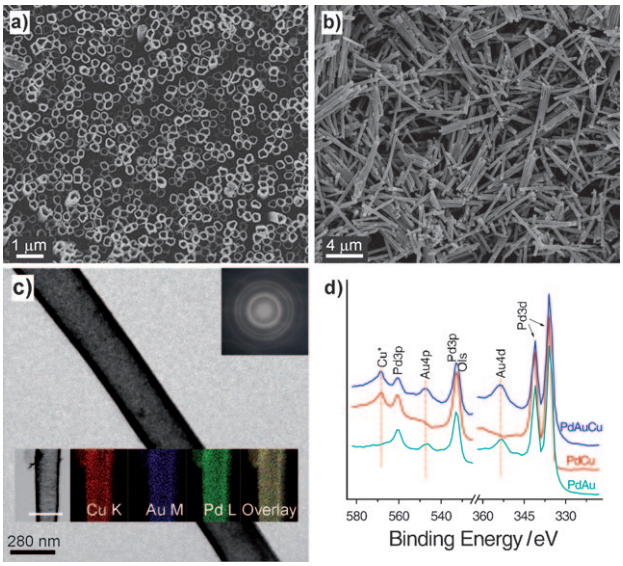

Figure 1. SEM images of PdAuCu HNTs showing the tubular (a) and well-dispersed (b) features. c) TEM image of a single PdAuCu HNT. Top inset: the electron diffraction pattern. Bottom inset: Montage showing the corresponding EDX maps of the Pd-L, Au-M, and Cu-K signals (Pd green, Au blue, Cu red; the overlay is a reconstructed PdAuCu HNT; inset scale bar is 500 nm). d) XPS scans of PdAuCu, PdCu, and PdAu HNTs; Cu* indicates the Auger line of Cu.

(TEM) image of the PdAuCu HNT shows the homogeneous wall thickness (Figure 1c). The tube wall is porous and consists of several layers of overlapped tiny particles, so the inner surfaces of the tubular catalyst are available as active sites (see Figure S1 in the Supporting Information). The size of the PdAuCu particles is about 2–6 nm, as revealed by the electron diffraction pattern (Inset in Figure 1c). The diffraction rings indicate small-size characteristics. For comparison, a PdCu nanoparticle tubular catalyst has also been prepared by the same route. The SEM and TEM images (see Figure S2 in the Supporting Information) indicate the PdCu has a tubular structure and the tube wall is thin enough for O_2 and H_2O_2 molecules to penetrate through it. From the amplified TEM image, even the particle-like rough surface morphology was also observed. The PdCu nanoparticle had an average size of 3.5 nm as indicated by the HRTEM image (see Figure S2 in the Supporting Information).

The PdAuCu HNTs was characterized by means of powder X-ray diffraction (XRD). The results clearly showed that the PdCu catalyst has a partial alloying phase without the addition of Au, and the reflection appeared at 41.5° for PdCu (111). Weak Pd diffraction peaks were also detected (see Figure S3 in the Supporting Information). In the whole process, the atom percentage of Cu was kept approximately 55% and always constant. When about 3 at.% by atom % of Au was introduced into the PdCu catalyst, the Au(111) and Au(200) diffraction peaks appeared as did Pd(311), and the relative intensity of characteristic PdCu(200) decreased. With the increase of atom percentage of Au to 21%, the diffraction peaks of PdCu become weak, but the diffraction peaks of Au and Pd become clear. This phenomenon can be explained by a phase equilibrium of the Pd-Au-Cu ternary system.[9] When the atom percentage of Cu was fixed at 55%, the introduction of Au changes the relative atom ratio of Pd, Au, and Cu, and moves the PdCu ratio outside that of the alloying phase isothermal section and the separated phase may form.

We further studied the surface composition of PdAuCu HNTs by X-ray photoelectron spectroscopy (XPS; Figure 1d). The strong signals from Pd3d and Au4d indicate the presence of Pd and Au. Because metallic Cu has low crystallinity and is absent in XRD patterns, the naked Cu/CuO was determined by energy position of the LMM Auger line of Cu (568 eV).[10]

Owing to the major reduction potential difference between Pd, Au, and Cu the preferential deposition may occur in this mixed Pd-Au-Cu ternary electrolyte solution. The energy-dispersive X-ray spectroscopy (EDX) maps were used to investigate elemental distributions and ratios of Pd, Au, and Cu metals (Figure 1c inset, and Figure S4 in the Supporting Information). The images reveal that the elements Pd, Au, and Cu are uniformly dispersed in PdAuCu HNTs. The elemental distribution also represents the homogeneous particle distribution. So the dispersed particle provide plenty of interface area with highly active sites.

The electrocatalytic properties of PdAuCu HNTs toward the oxygen reduction reaction (ORR) along with those of PdCu and PdAu HNTs, and the commercial Pt/C catalysts (Johnson-Matthey, 20 wt%) have been investigated. Figure 2a shows the cyclic voltammogram (CV) curves. It shows that both the PdCu and PdAu have lower intensity redox waves than the PdAuCu catalyst. The redox waves of

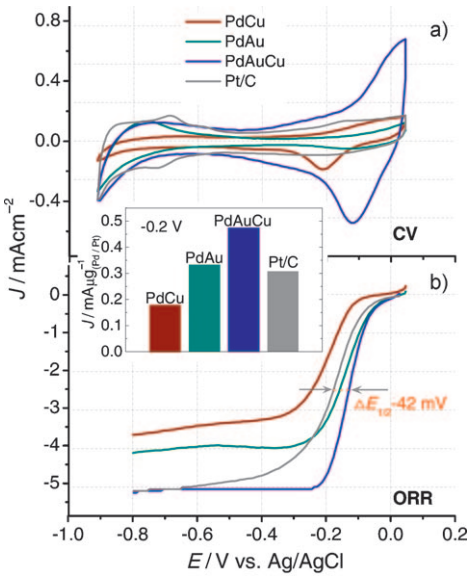

Figure 2. a) CV curves recorded in Ar-purged 0.1 M KOH solution at room temperature with a sweep rate of 50 mV s^{-1}. b) ORR polarization curves for PdCu, PdAu, PdAuCu HNTs, and Pt/C catalysts. Inset: the mass activity at −0.2 V for these four catalysts.

PdAuCu and PdCu appears at −0.12 and −0.21 V assigned to the reduction reaction of Cu^{2+} to Cu^{+} and Cu^{+} to Cu,[11] which indicates that the introduction of Au can lower the oxidation potential of Cu and favor the formation of active Cu^{II} species through the potential difference of Au/Cu system. Moreover, this CuO can be easily transformed to Cu under the negative CV reducing treatment. Undoubtedly, the presence of Cu^{II} species can improve the catalytic properties toward ORR, but whether this enhancement is due to Cu^{2+} mediators,[11] or arises from adsorption sites to increase the concentration of O_2 over the cathode[12] is still controversial. In our experiment, the Cu^{II} species can form under lower potential in the presence of Au, demonstrating that both adsorption site and mediator function can occur (see Figure S5 in the Supporting Information).

The ORR measurements (Figure 2b) were performed in O_2 saturated 0.1M KOH solutions at room temperature using a glassy carbon rotating disk electrode with a sweep rate of 50 mV s^{-1} at 1600 rpm. For the PdAuCu, PdCu, PdAu, and Pt/C catalysts, the low metal loading of Pd or Pt was 10.2 μg cm^{-2}. The PdAuCu electrode showed an onset potential of 0 V, a shift of about 0.1 V to more positive potential than for the PdCu electrode, and the diffusion-limiting current from −0.8 to −0.25 V is very steady and nearly twice that of PdCu (the current density for PdAuCu at −0.2 V (vs. Ag/AgCl, if not specified otherwise.) reaches 4.75 mA cm^{-2}, nearly three times than that of PdCu (1.75 mA cm^{-2}), indicating the accelerated ORR kinetics caused by Au. The PdAu electrode for ORR has similar onset potential to PdAuCu, but the diffusion-limiting current is also lower, indicating that the

enhanced catalytic activity of PdAuCu cannot be achieved by just Au or Cu. Comparing this PdAuCu catalyst with the Pt/C catalyst, the half-wave potential for ORR shifts towards more positive potential by 42 mV. Moreover, PdAuCu has the highest mass activity and even 2.7 times higher than that of PdCu and 1.6 times than that of Pt/C (Figure 2, inset). The improved activity of the PdAuCu catalyst for ORR might be due to the change of electronic structure and local reactivity of the surface in complex and mixed particle interfaces,[13] the presence of Cu^{II} species formed at lower potential[11,12] (see Figure S5 in the Supporting Information), and oxygen incorporation at the metal/oxide interface.[14]

The formation of hydrogen peroxide (H_2O_2) as an intermediate in ORR is the main energy loss on using gaseous O_2 as the oxidant, suggesting that H_2O_2 cannot be used directly as a liquid oxidant for fuel-cell applications because the HO_2^- reduction occurs only with large overpotentials. We investigated the catalytic activity of PdAuCu towards H_2O_2 reduction (HR) in argon-saturated 0.1 M KOH aqueous solution (Figure 3a). The CV curves are very similar to those obtained for the ORR, which means H_2O_2 can also serve as an oxidant for fuel-cell applications and exhibit a high limiting current. For PdAuCu the trace is approximately a straight line from −0.8 to −0.25 V like for the ORR CV curves. At the present stage, the measured similar CV curves (with the oxygen-reduction current at the mixed kinetic-diffusion control region between −0.25 and −0.08 V) in the HR reaction, which are similar to the ORR reation, are due to the catalytic decomposition of H_2O_2 and the high absorption of, and the reduction of, the in situ produced O_2. The high catalytic activity toward ORR of the PdAuCu catalyst as the mentioned above plus the unique decomposition of H_2O_2 and adsorption of O_2 induced the indirect reduction of the overpotential of the H_2O_2 reduction. The unique enhanced catalytic activities of PdAuCu may be due to the polarization effect at the noble metal and metal oxide interface.[15]

For fuel-cell applications, we also performed the investigation of the stability and durability of these catalysts in argon-saturated 0.1 M KOH aqueous solution (Figure 3a). The Pt/C catalyst has a drastic decrease even at the initial several circles. The PdCu catalyst is also somewhat unstable but has a higher reduction current, conversely PdAu is very stable but has a lower current. The PdAuCu catalyst shows synergistic effects from combining PdCu and PdAu catalysts, it is both stable and has a higher current. To evaluate the long-term electrocatalytic performance, the chronoamperograms (current–time profiles) of these catalysts were recorded with a bias at −0.2 V in argon-saturated 0.1 M KOH solution with 7.84 mM H_2O_2 (Figure 3b). It is clear that the Pt/C electrode in H_2O_2 solution undergoes accelerated corrosion and causes the degradation of Pt/C catalyst (*J* becomes less negative). As a result of the stabilization characteristics of Au towards ORR,[16] and as found in our case for the HR reaction, the long-term catalytic ability of the PdAuCu catalyst has been improved from 4 to 6 mA cm^{-2} compared to PdCu catalyst.

In conclusion, the as-synthesized PdAuCu HNT dual catalyst provides a promising route to the development of next-generation of mixed gas/liquid oxidant fuel cells with ultra-high electrical power output. The dual catalyst takes advantage of its unique catalytic properties for the HR reaction with an overpotential as low as for ORR. This PdAuCu HNT dual catalyst architecture also provides a new understanding of the synergistic effect, and consequently helps in designing new electrocatalysts with excellent stability and durability.

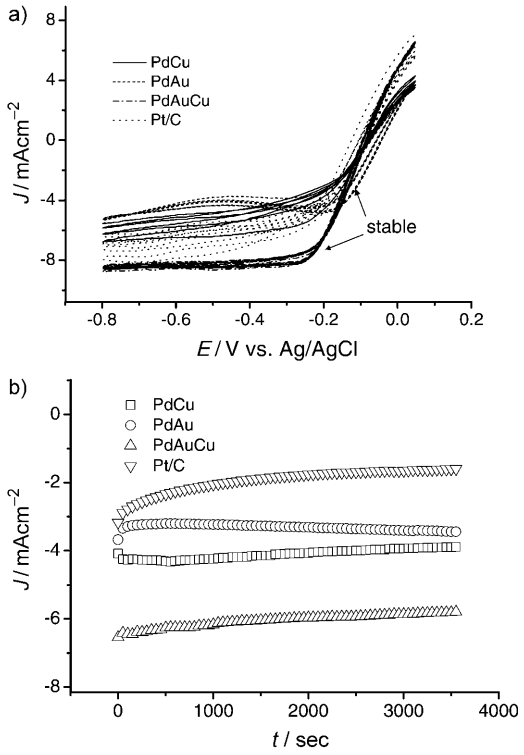

Figure 3. a) CV curves of the initial scans and b) the corresponding current (*J*) versus time (*t*) chronoamperometric curves obtained for H_2O_2 reduction using PdCu, PdAu, PdAuCu HNTs, and Pt/C catalysts.

Received: May 29, 2010
Revised: August 22, 2010
Published online: October 21, 2010

Keywords: electrocatalysis · electrodeposition · fuel cells · nanoparticles

[1] a) A. Chen, P. Holt-Hindle, *Chem. Rev.* **2010**, *110*, 3767; b) C. Bianchini, P. K. Shen, *Chem. Rev.* **2009**, *109*, 4183.
[2] W. P. Zhou, X. Yang, M. B. Vukmirovic, B. E. Koel, J. Jiao, G. Peng, M. Mavrikakis, R. R. Adzic, *J. Am. Chem. Soc.* **2009**, *131*, 12755.
[3] a) B. Lim, M. Jiang, P. H. C. Camargo, E. C. Cho, J. Tao, X. Lu, Y. Zhu, Y. Xia, *Science* **2009**, *324*, 1302; b) Z. M. Peng, H. Yang, *J. Am. Chem. Soc.* **2009**, *131*, 7542; c) H. Lee, S. E. Habas, G. A. Somorjai, P. Yang, *J. Am. Chem. Soc.* **2008**, *130*, 5406.
[4] a) M.-H. Shao, K. Sasaki, R. R. Adzic, *J. Am. Chem. Soc.* **2006**, *128*, 3526; b) V. R. Stamenkovic, B. Fowler, B. S. Mun, G. F. Wang, P. N. Ross, C. A. Lucas, N. M. Markovic, *Science* **2007**, *315*, 493; c) R. Srivastava, P. Mani, N. Hahn, P. Strasser, *Angew. Chem.* **2007**, *119*, 9146; *Angew. Chem. Int. Ed.* **2007**, *46*, 8988; d) V. Mazumder, M. Chi, K. L. More, S. H. Sun, *J. Am. Chem. Soc.* **2010**, *132*, 7848.

[5] a) M. Valden, X. Lai, D. W. Goodman, *Science* **1998**, *281*, 1647; b) D. Matthey, J. G. Wang, S. Wendt, J. Matthiesen, R. Schaub, E. Laegsgaard, B. Hammer, F. Besenbacher, *Science* **2007**, *315*, 1692; c) J. H. Kwak, J. Hu, D. Mei, C. W. Yi, D. H. Kim, C. H. F. Peden, L. F. Allard, J. Szanyi, *Science* **2009**, *325*, 1670; d) W. E. Kaden, T. Wu, W. A. Kunkel, S. L. Anderson, *Science* **2009**, *326*, 826; e) A. A. Herzing, C. J. Kiely, A. F. Carley, P. Landon, G. J. Hutchings, *Science* **2008**, *321*, 1331; f) D. I. Enache, J. K. Edwards, P. Landon, B. Solsona-Espriu, A. F. Carley, A. A. Herzing, M. Watanabe, C. J. Kiely, D. W. Knight, G. J. Hutchings, *Science* **2006**, *311*, 362; g) M. S. El-Deab, T. Ohsaka, *J. Electrochem. Soc.* **2008**, *155*, D14; h) J. B. Park, J. Graciani, J. Evans, D. Stacchiola, S. D. Senanayake, L. Barrio, P. Liu, J. F. Sanz, J. Hrbek, J. A. Rodriguez, *J. Am. Chem. Soc.* **2010**, *132*, 356; i) M. S. El-Deab, T. Ohsaka, *Angew. Chem.* **2006**, *118*, 6109; *Angew. Chem. Int. Ed.* **2006**, *45*, 5963.

[6] C. H. Cui, H. H. Li, S. H. Yu, *Chem. Commun.* **2010**, *46*, 940.

[7] Y. W. Lee, M. Kim, Z. H. Kim, S. W. Han, *J. Am. Chem. Soc.* **2009**, *131*, 17036.

[8] Z. W. Chen, M. Waje, W. Z. Li, Y. S. Yan, *Angew. Chem.* **2007**, *119*, 4138; *Angew. Chem. Int. Ed.* **2007**, *46*, 4060.

[9] T. Morimura, S. Matsumura, M. Hasaka, H. Tsukamoto, *Philos. Mag. A* **1997**, *76*, 1235.

[10] Z. Mekhalif, F. Sinapi, F. Laffineur, J. Delhalle, *J. Electron Spectrosc. Relat. Phenom.* **2001**, *121*, 149.

[11] H. Watanabe, H. Yamazaki, X. Y. Wang, S. Uchiyama, *Electrochim. Acta* **2009**, *54*, 1362.

[12] Y. Nabae, I. Yamanaka, K. Otsuka, *Appl. Catal. A* **2005**, *280*, 149.

[13] S. Tanaka, N. Taguchi, T. Akita, F. Hori, M. Kohyama, *Solid State Phenom.* **2008**, *139*, 47.

[14] T. Schalow, M. Laurin, B. Brandt, S. Schauermann, S. Guimond, H. Kuhlenbeck, D. E. Starr, S. K. Shaikhutdinov, J. Libuda, H. J. Freund, *Angew. Chem.* **2005**, *117*, 7773; *Angew. Chem. Int. Ed.* **2005**, *44*, 7601.

[15] a) Y. Lee, Miguel A. Garcia, Natalie A. Frey Huls, S. Sun, *Angew. Chem.* **2010**, *122*, 1293; *Angew. Chem. Int. Ed.* **2010**, *49*, 1271; b) C. Wang, H. Daimon, S. Sun, *Nano Lett.* **2009**, *9*, 1493.

[16] J. Zhang, K. Sasaki, E. Sutter, R. R. Adzic, *Science* **2007**, *315*, 220.

